BG Pulse Journal USA
ISSN:1947-2536 http://www.bgpulseusa.com/index.php/bg

STATIC AND DYNAMIC CHARACTERISTICS OF OPTOELECTRONIC DISCRETE CONVERTERS FOR AUTOMATIC MEASUREMENT OF DISPLACEMENTS AND DIMENSIONS

Kholmatov Umid Sadirdinovich
Associate Professor of the Department of "Transport Logistics" of Andijan State Technical Institute, Uzbekistan, Andijan,
E-mail: umid.xolmatov.76@mail.ru.
https://orcid.org/0000-0003-2295-502X
Doi: https://doi.org/10.5281/zenodo.21545019

Abstract: This article shows the static and dynamic characteristics of optoelectronic discrete displacement transducers, as well as the reliability of optoelectronic discrete displacement transducers with hollow and fiber light guides. Optoelectronic converters based on hollow and fiber light guides, due to their simple and reliable designs, cost-effectiveness and manufacturability, are widely used for automation in various production processes. Among optoelectronic converters based on hollow and fiber light guides, discrete converters for the level of liquids, the inclination of various objects, devices for automatic counting of piece products on conveyor lines, and others have not been sufficiently developed and studied. Optoelectronic converters based on hollow and fiber light guides are compatible with microprocessors and are capable of efficiently and discretely converting various physical quantities that, at the input of the converter, changing the parameters of the light flux as it propagates from the source to the radiation receiver. The challenge of developing and refining optoelectronic discrete converters based on hollow and fiber light guides (ODC) that satisfy contemporary monitoring and control system requirements greatly advances the field's understanding of optoelectronic converters based on ODCs as well as monitoring and control systems for a range of technological processes.

Key words: liquid level, optical fibers, reflective modulating element, multifunctionality, sources and receivers of radiation, signaling relay circuit.

Introduction. The priority directions for the implementation of the new development strategy of Uzbekistan for 2022-2026, including the active introduction of green economy technologies in all sectors, set the task of increasing the energy efficiency of the economy by 20% by 2026 and reducing the volume of harmful gases emitted into the air by 20%. Technical and technological improvement is considered important in accomplishing this task.

Due to the need to improve the efficiency of production processes and the development of automated monitoring and control systems, the importance of converters used to obtain information about various parameters of technological processes is constantly increasing.

Currently, significant changes are taking place in the development of the integration of automated control systems and information systems. This is due to the achievements of microelectronics, microprocessor and computer technology, new processes and phenomena of semiconductor, solid-state and film technology, as well as the use of new materials [1, 2, 4, 7, 8, 16].

Optoelectronic converters are very promising for measuring the displacements and sizes of various objects, including granules of materials from the mining and processing industries of the food industry: tubers, grain, seeds, grinding, etc. Among optoelectronic converters, converters

BG Pulse Journal USA
ISSN:1947-2536 http://www.bgpulseusa.com/index.php/bg

based on hollow fibers have not been sufficiently studied and developed, which, when using ring radiation receivers with concentrated radiation sources located symmetrically along the axis of a hollow fiber, allow measuring small displacements with high sensitivity and accuracy with continuous automatic control [2, 3, 9, 13, 15, 17].

Methods

An optoelectronic converter based on a hollow fiber (Figure 1) consists of a concentrated radiation source *1*, a hollow fiber *2*, a radiation receiver *3* and a longitudinal moving reflective disk *4*, which modulates the light flux $\Phi_0(x)$ when moving and is rigidly connected to the rod *5*, on which is affected by displacement x_0. The light flux $\mathbf{\Phi_0}$, propagating from the radiation source *1*, located at a distance x_0 from the radiation receiver *3*, and passing through the hole, falls on the light-sensitive surface of the disk *4* and further, reflected from it, onto the light-sensitive surface of the radiation receiver *3*.

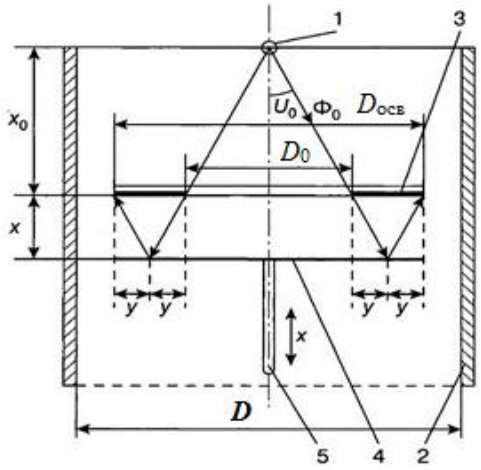


Figure 1. Physical model of an optoelectronic displacement transducer: *1*-concentrated radiation source; *2*-hollow LED; *3*-radiation receiver; *4*-length reflective disk; *5*-rod.

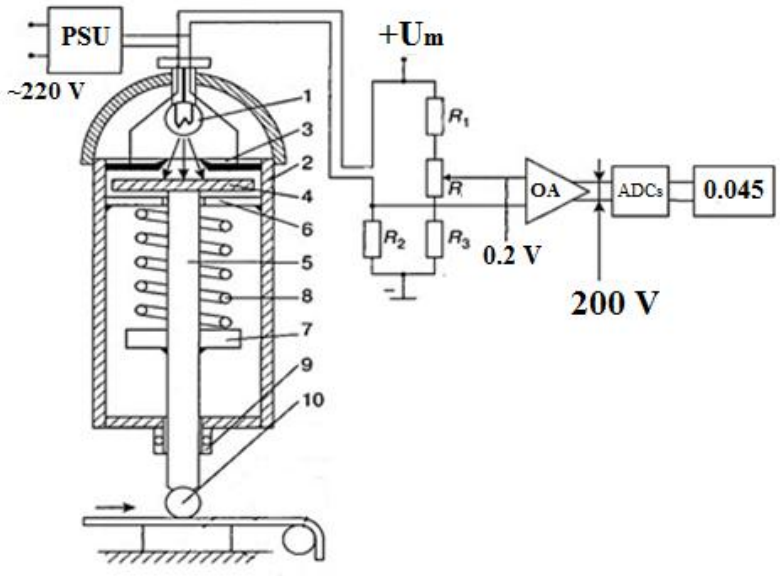


Figure 2. The design and measuring circuit of the optoelectronic displacement transducer: *1*-radiation source (incandescent bulb); *2*-hollow fiber; *3*-ring photoresistor; *4*-reflective disc; *5*-rod; *6* and *7* stops; *8*-spring; *9*-guide tip; *10*-roller.

In figure 2. the design and measuring scheme of an optoelectronic converter for automatic control of the thickness of tape materials that are transported using coils or other devices are presented. In order to control the thickness of the tape material 12, the optoelectronic converter is set to a certain thickness (nominal), which is determined by the standard and the requirements for the measured material. During measurement, thickness (size) deviations are automatically captured and the transducer output signal is used to automatically control the material thickness [1, 2, 5].

Results and discussion

Dynamic characteristics of optoelectronic discrete displacement transducers.

The dynamic characteristic of the ODC corresponds to an aperiodic link of the first order and will significantly manifest itself when the measured value fluctuates (liquid level and during displacements) at high speed.

For example, let the fluctuations in the liquid level occur according to a sinusoidal law:

$$H(t)=H_0+H* \ sin\omega t \tag{1}$$

Then the output parameter of the ODC will change according to the law:

$$R_{PR1}(t)=R_{PR1}+\frac{R_{PR1}}{\sqrt{1+(T\omega)^2}}* \ sin(\omega t-f) \tag{2}$$

If in ODC designed to control the liquid level TFL (the time constant of the float or liquid surface) is much greater than the time constant of the radiation receiver T_{RR} $T_{LS} \gg T_{RR}$, then the dynamic characteristic of such TFL will not have a significant impact on the result of level measurement. By analogy with expression (6), at a high pulse repetition rate w, the amplitude of the output signal in accordance with (6) and can be reduced by $1+T^2\omega^2$ times, and the phase is shifted by an angle $f=arctgT\omega$ when counting a sequence of pulses, taking into account piece products, disk rotation speed and others [1, 2].

It is known that the time constant T_{PR} of photoresistors depends on the illumination and on the time they are kept in the dark. With a long exposure of the photoresistors in the dark, the time constant of the rise of the photocurrent Tfrn increases by 3-4 times. For photodiodes, the time constant is determined by the expression

$$T_{PR}=R_R* \ C* \ (1+\beta_{Ph}* \ R_R) \tag{3}$$

where: R_R - load resistance, C - capacitance p-n - transition; β_{Ph} is the conversion factor of the feedback link in the block diagram of the photodiode.

The values of the time constants for photoresistors is $T_{PD}=0.08-0.2\ s$, and for photodiodes $T_{PD}=10^{-5}s$.

In ODC with transverse movement of the moving element with instantaneous illumination of the entire photoresistor, the increase in the light current $I_c(t)$ occurs according to the expression

$$I_C(t)=I_H+I_{PC}* \ (1-e^{-\frac{t_H}{T_H}}), \tag{4}$$

where: I_H I_{PC} are the dark and photocurrent of the photoresistor, respectively; t_H, T_H are, respectively, the rise time of the photocurrent I_{PC}. With instantaneous partial illumination of a completely darkened photoresistor, the current rise is determined from the expression

$$I_{FIH}(t)=\frac{m*\ U}{R_T\left[K_c(1-m)\left(1-e^{-\frac{t_H}{T_H}}+m\right)\right]+m*\ R_H}, \quad (5)$$

and the current decay with sequential dimming of the photoresistor

$$I_{FIRP}(t)=\frac{m*\ U}{R_T\left[K_т(m-1)\left(1-e^{-\frac{t_{RP}}{T_{RP}}}+1\right)\right]+m*\ R_H}, \quad (6)$$

where: $K_C=\frac{S_C}{S}$ is the ratio of the illuminated part to the entire area of the photoresistor; t_{RP}, T_{RP} are, respectively, the decay time and the decay time constant of the photocurrent; U is the circuit voltage; m is the ratio of the dark resistance to the light resistance of the photoresistor.

Investigation of errors in optoelectronic discrete displacement transducers with hollow and fiber light guides.

The errors of the ODC can be classified according to different criteria:

1) according to the degree of uncertainty;
2) depending on the conditions of work;
3) depending on the source and causes of occurrence, etc.

According to the degree of uncertainty, errors are divided into systematic and random, and depending on the operating conditions - into basic and additional.

It is advisable to estimate the total error of the ODC based on the position of the information theory of measuring devices, from the point of view of which the error of measuring devices is uniquely determined by the value of the entropy error (Δ_e), and the entropy coefficient K_e depends on the form of the probability density distribution law of element errors.

$$\Delta_e=K_\sigma*\ \sigma_\Sigma$$

The expression yields the value of the total root-mean-square error σ_Σ for ODC, which has "n" elements.:

$$\sigma_2=\sqrt{\sigma_1^2+\sigma_2^2+\ldots+\sigma_i^2+\sigma_n^2} \quad (7)$$

σ_i - root-mean-square error of the i -th element of the ODC.

Let us determine the calculated value of the ODC error on the basis of the structural diagram. The main elements of the ODC are analyzed below from the point of view of possible sources of errors: photoresistor (PR); bridge measuring circuit (MC); operational amplifier (ADCs) and relay (Re) of the measurement results y k.

The limiting number $\gamma_{PR}=0.2\%$ normalizes the additive error of PR. A bridge measurement circuit, which has an additive error of $y_{MC}=0.1\%$, is linked to the PR.

The measuring circuit is powered by a stabilizer (ST), which, together with the amplifier, is powered by a common power supply unit (PSU). An operational amplifier is used as ADCs, which linearizes the static characteristic and has a large input impedance. The output element of the ODC is an electromagnetic relay.

Firstly, we will split up all of the error's components into additive and multiplicative ones. Then, we will find each component's root-mean-square deviation based on the distribution law. Every computation is done using the relative values provided, and one extra inaccurate decimal place is added to the data during intermediate rounding [2, 5, 10, 12, 14].

Let the multiplicative error caused by variations in the supply voltage of the MC and ADCs, the additive errors of the PR, MC, and Re, and the temperature dependency of the sensitivity of the amplifier (ADCs) and relay (Re) account for the additive error of the total converter set. The

distribution law of the PR error can be interpreted as normal, given an entropy value of K_{PR}=2.07. The standard deviation (RMSD) from this point on is equal to

$$\sigma_{PR}=\frac{\gamma_{PR}}{K_{PR}}=\frac{0.2}{2.07}=0.097\% \quad (8)$$

Similarly, for the measuring circuit with the normal law of error distribution we have:

$$\sigma_{MC}=\frac{0.2}{2.07}=0.048\ \% \quad (9)$$

The standard specifies that an allowance for aging is included in the indication of electromagnetic relay inaccuracy. Thus, the value $\gamma_{Re}=0.8\,\gamma_k$, where γ_{Re} is the main error corresponding to the accuracy class, can be used to determine the maximum error Re.

$\gamma_{Re}=0.8*\ 0.5=0.40\%$. from here on. With an entropy coefficient of K_{yk}=1.9, the law governing the distribution of mistakes in electromechanical devices is nearly trapezoidal. Consequently, we get $\sigma_{Re}=\frac{\gamma_{Re}}{1.9}=\frac{0.40}{1.9}=0.21\%$. The total of the three elements will determine the additive error of the device. As a result, the zero ODC RMS error will be:

$$\sigma_н=\sqrt{\sigma_{PR}^2+\sigma_{MC}^2+\sigma_{Re}^2}=\sqrt{0.097^2+0.048^2+0.21^2}=0.236\% \quad (10)$$

The graphs showing how the entropy coefficients rely on the respective weights of the dispersion must be consulted in order to calculate the entropy coefficient of the total of these errors [1, 2, 6, 18].

$P=\frac{\sigma_{Re}^2}{\sigma_н^2}=\frac{0.21^2}{0.236^2}=0.79$ is the relative weight of the dispersion of the trapezoidal distribution in the total dispersion. The value of P in this instance is K_a=2.0. The entropy value of the ODC's mistake of zero will thus be as follows:

$\gamma_н=K_н*\ \alpha_н=2.00*\ 0.236=0.47\%$ (11)

We now take the following beginning data and turn to the summing of multiplicative mistakes. Let $\varphi_{Re}=0.2\%\ 10^0K$ be the coefficient of influence of temperature on the sensitivity Re, and let $\varphi_{Re}=0.1\%\ 10^0K$ be the amplifier.

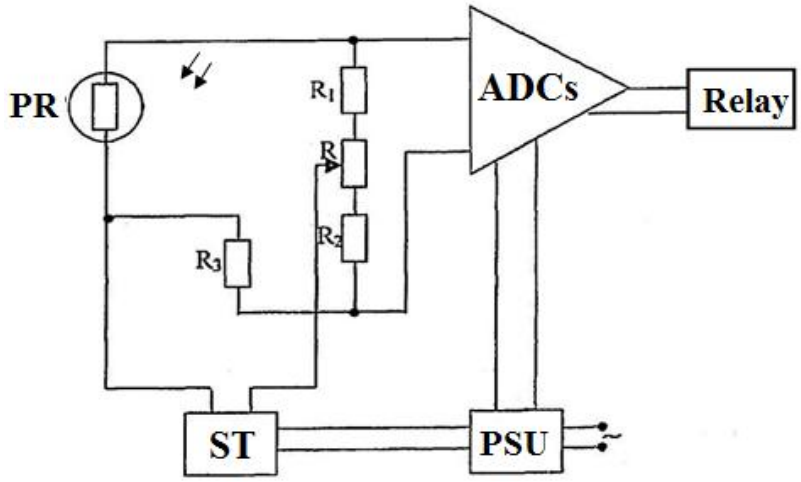


Figure 3. Measuring circuit of the ODC.

BG Pulse Journal USA
ISSN:1947-2536 http://www.bgpulseusa.com/index.php/bg

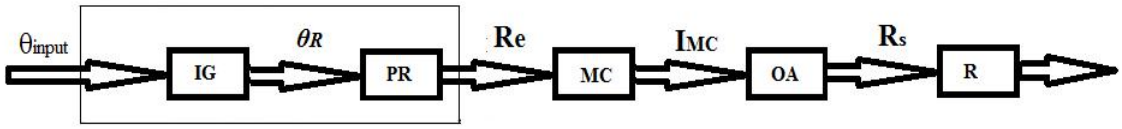


Figure 4. Structural diagram of the ODC.

Assume for the moment that the ODC is designed to operate under workshop circumstances at temperatures between +5 and +35 °C, or 20 ± 15 °C, and that all temperatures are equally likely. The multiplicative error's temperature component then has a uniform distribution [1, 2, 10].

$$\gamma_{\theta M}=0.1*\ \frac{15}{10}=0.15\% \tag{12}$$

and

$$\sigma_{\theta}=\frac{\gamma_{\theta}}{K_{\theta}}=\frac{0.15}{1.73}=0.087\% \tag{13}$$

Let the voltage variations of the network that powers the considered ODC have a triangle probability distribution law and be within ±10%. A stabilizer with a stabilization factor of K=25 powers the IC. Then, within the bounds $y_{MC}=\frac{10}{25}=0.40\%$ with RMS, the oscillations in the IC's supply voltage and, subsequently, the multiplicative error of its output voltage, likewise have triangle distributions:

$$\sigma_{ES^1}=\frac{\gamma_{ES}}{\sqrt{6}}=\frac{0.4}{\sqrt{6}}=0.163\% \tag{14}$$

ADCs is powered by an unstabilized voltage, but due to deep negative feedback, the coefficient of influence of the supply voltage on the gain is reduced to the value $\Psi_{\theta G}=\frac{0.3}{[10\left(\frac{\Delta U}{U}\right)]}$. As a result, a triangle rule will likewise govern the distribution of the multiplicative error of the ODC, which is brought on by sporadic variations in the supply voltage, inside $y_{ES}=\pm 0.30\%$ with RMS

$$\sigma_{ES^2}=\frac{\gamma_{ES}}{\sqrt{6}}=0.3\sqrt{6}=0.122\% \tag{15}$$

Since both voltage fluctuation errors are caused by the same cause, they are correlated with each other and add up algebraically, not geometrically, although each of them is random. That's why:

$$\begin{gathered} y_S=y_{ES}+\gamma_{\theta M}=0.3+0.4=0.7\% \\ \sigma_S=\sigma_{ES^2}+\sigma_{ES^1}=0.122+0.163=0.285\% \end{gathered} \tag{16}$$

Because temperature and voltage fluctuation mistakes are independent of one another, they add up geometrically, that is, with the multiplicative component's RMS.

$$\sigma_M=\sqrt{\sigma_s^2+\sigma_{\theta}^2}=\sqrt{0.285^2+0.087^2}=0.298\% \tag{17}$$

The criteria for summing independent mistakes state that the total error of the ODC is equal to the sum of the additive and multiplicative errors:

$$\sigma_{\Sigma}=\sqrt{\sigma_H^2+\sigma_M^2}=\sqrt{0.236^2+0.298^2}=0{,}38\% \tag{18}$$

The RMS of the aggregated errors K_H=2.00 and K_M=2.04 are near to each other, and their entropy coefficients are fairly significant.

$$\sigma_н=0.236 \quad and \quad \sigma_м=0.298 \tag{19}$$

therefore, we can conclude that the overall entropy coefficient K_Σ=2.07

and $\Delta_{ODC}=2.07* 0.38=0.79\%$ (20)

Thus, it is possible to accept the accuracy class of the ODC as not exceeding 1.0%.

Reliability of optoelectronic discrete displacement transducers with hollow and fiber light guides.

Table 1. Types of mechanisms and causes of failure of optoelectronic elements of the ODC.

Types of failures	Failure mechanisms	Reasons for refusals
Degradation of the spectrophotometric parameters of emitters	Degradation of the internal quantum yield, increase in the concentration of nonradiative recombination centers, diffusion of impurities and defects to the transition	Overcurrent, ionizing radiation, defects in the bulk of the semiconductor, mechanical impact on the crystal
	Aging of optical media materials, reduction of light transmittance	Excess temperature, thermal aging of polymers, ionizing radiation
	Deflection of optical media from the crystal, change in light transmittance	Exceeding the temperature gradient, non-compliance of materials according to the CTE
Increasing the dark current of the photodetector	Accumulation of charge on the surface of the photodetector, inversion of the sign of conductivity	The presence of moisture and dirt inside the case, leakage
Breakage of wire connections	Mechanical forces arising from temperature changes, fatigue phenomena	Exceeding the temperature gradient, mismatch of materials according to CTE, low bond strength
	Metallization corrosion	The presence of moisture and dirt inside the case, leakage
	Electromitation	Electric overload
	Breakage due to mechanical influences	Exceeding the limits of resistance to mechanical stress, low strength connections

The reliable operation of the ODC is influenced by the parameters and characteristics of emitters, optical connectors, cable, and photodetector. To obtain optimal matching of the emitter with an optical fiber, it is necessary that the emitter meets a number of requirements. This is, first

of all, a small radiating area, commensurate with the diameter of the fiber, which provides a high energy brightness of the source; wavelength of radiation corresponding to the minimum absorption of light when it passes through the fiber; the possibility of simple docking of the emitter with the fiber; preservation of radiating characteristics in a given temperature range and storage of the product under the influence of various mechanical factors [1, 10].

The main parameter when connecting radiation sources with optical fibers is the radiation input coefficient $\eta=\eta_S * \eta_\varphi$, where $\eta_S=\frac{S_F}{S_s}$ is the radiation input coefficient over the area;

$$\eta_\varphi=\frac{\int_0^{\theta_{Kp}} Q_v(\theta)sin\theta d\theta}{\int_0^{\pi/2} Q_v(\theta)sin\theta d\theta} \quad (21)$$

1 - coefficient of input of radiation in angle; S_F is the cross-sectional area of the fiber; S_s - area of the radiating area of the diode: $Q_v(\theta)$ - light energy; θ is the angle.

The radiation power injected into the fiber depends strongly on the numerical aperture of the fiber:

$$P_{IG}=F_y\left(\frac{n+1}{2}\right)\frac{S_{FCA}}{S_{ES}}(NA)^2P_{ES}, \quad (22)$$

where: P_{IG} is the radiation power introduced into the fiber; P_{MCT} is the power emitted by the source; F_y - fill factor; S_{FCA} is the area of the fiber core; S_{ES} is the active area of the source, n is the indicator of the radiation pattern $(cos * \theta)^n$; $NA=n * sin\theta=(n^2 2-n^2 1)^{\frac{1}{2}}$ - numerical aperture; n_1 is the refractive index of the fiber cladding; n_2 is the refractive index of the fiber core.

NA values are usually in the range of 0.15-0.50. With an increase in NA, the dispersion for LEDs increases, which limits the practically achievable values of the radiation input efficiency when using the maximum possible value of n.

The exponent n for light-emitting diodes is equal to one, and for lasers and LEDs with built-in lenses, the value of n can take values of *2–4*, since injection lasers have narrowed radiation patterns. It is also possible to increase the input coefficient of LED radiation by changing the geometry of the emitter. The emitter output power is concentrated in a beam with angular dimensions of 120°×40° (for diodes with an active edge surface) or corresponds to the Lambertian radiation pattern (for diodes with an active flat surface) [2, 5, 12].

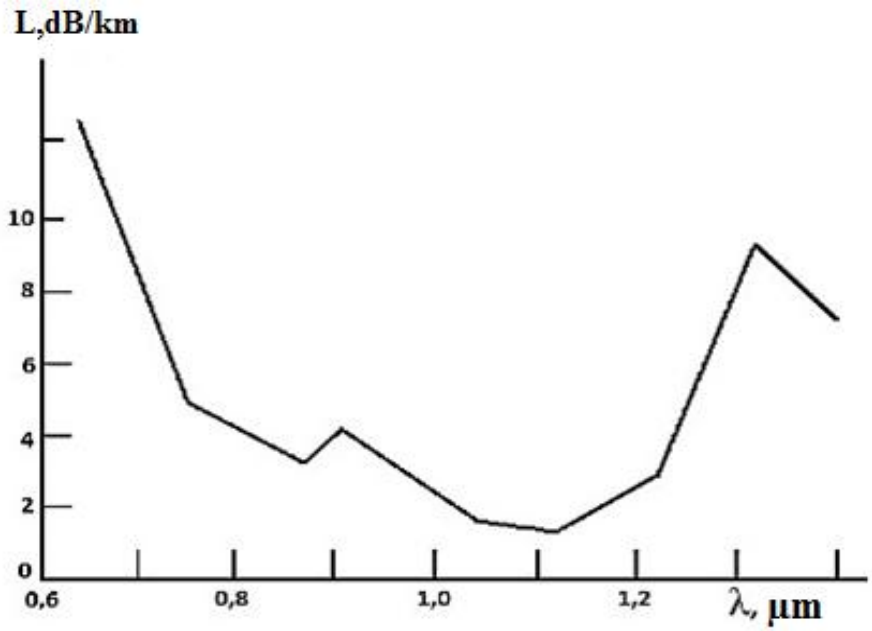


Figure 5. Signal attenuation curve in glass fiber for various wavelengths.

The losses for the input of radiation into an optical fiber reach a significant value, for example, for an optical fiber with a numerical aperture of 0.14, the losses are about 14 dB for emitters with input of radiation along the *p-n* junction (edge emitters) and 19 dB for surface emitters. Edge emitters provide higher fiber coupling efficiency than active flat surface diodes, but the lower fiber coupling efficiency is more than offset by their higher radiation power. In general, the reliability of optoelectronic discrete converters with respect to gradual failures, taking into account the operating factors, with an error of not more than 1.0%, is equal to

$$P=\Phi\left(\frac{\Delta S_{max}}{G_s}\right)-\Phi\left(\frac{\Delta S_{max}}{G_s}\right)=\Phi\left(\frac{1}{0.45}\right)-\Phi\left(-\frac{1}{0.45}\right)=0.97, \quad (23)$$

where: the ratio of the allowable sensitivity ΔS to the maximum sensitivity is

$$\frac{\Delta S}{S_{max}}=0.45 \quad (24)$$

Conclusion. The static characteristics of optoelectronic discrete converters are determined on the basis of a joint consideration of the designs of converters with hollow and fiber light guides and the corresponding measuring circuit with a radiation receiver. It is shown that dividing and bridge measuring circuits are mainly used in optoelectronic discrete displacement transducers.

The static characteristics of relay optoelectronic discrete converters with lumped radiation sources based on hollow and fiber light guides are obtained for longitudinal and transverse displacements of the external modulating body.

The dynamic characteristics of optoelectronic discrete displacement transducers can be described by a first-order aperiodic link, and the curves of the change in the shape of the output signals of discrete transducers significantly depend on the mixing speed of the controlled volume, liquids, piece products and materials.

The reliability of optoelectronic discrete displacement transducers is ensured by the indicator of the sensitivity value in the tolerance field, taking into account the existing factors, and with an allowable error of 1.0%, they will be 0.97%.

The entropy value of the error of discrete optoelectronic displacement transducers is Δ_e=0.79 %, which does not exceed the accuracy class of 1.0%.

References

1. Kholmatov, U. S., Mukimova, D. K., Xalimjonov, E. X., Soliyev, A. F., Maribjonov, M. M., Komilov, M. R., & Shukurov, M. (2024). Characteristics of optoelectronic discrete displacement converters with hollow and fiber light guides. In E3S Web of Conferences (Vol. 471, p. 06015). EDP Sciences.
2. Kholmatov, U. (2022). Intelligent discrete systems for monitoring and control of the parameters of technological processes on the basis of fiber and hollow fiber. Monograph.–2022.–C, 5-114.
3. Rayimdjanova O. et al. Practical approach to aspects of operation and practical use of optoelectronic linear transducer of movements of the first hazard category objects //E3S Web of Conferences. – EDP Sciences, 2023. – T. 452. – C. 01011.
4. Nurdinova, R., Rayimjonova, O., Djalilov, B., & Iskandarov, U. (2024, March). Determination of the near areas of micro parameters for anomalous photo voltage elements. In AIP Conference Proceedings (Vol. 3045, No. 1). AIP Publishing.
5. Kholmatov, U. (2022). DETERMINATION OF THE MAIN CHARACTERISTICS OF OPTOELECTRONIC DISCRETE DISPLACEMENT TRANSDUCERS WITH HOLLOW AND FIBER FIBER. SCIENTIFIC AND TECHNICAL JOURNAL MACHINE BUILDING, (4), 160-168.
6. Kholmatov, U. S. (2022). Determination of the basic and static characteristics of optoelectronic discrete displacement transducers with hollow and fiber light. SCIENTIFIC AND TECHNICAL JOURNAL OF MECHANICAL ENGINEERING.–2022, 5, 711-719.
7. Khayrullo Baynazarov, Shoyadbek Turayev, Abdumannob Giyasidiniv, Sarvarbek Ismailov, Nurmuxammad Maxammadjonov, and Xasanboy Sotvoldiyev. Calculation for variations in resistance force during trailer unloading device operation E3S Web of Conferences 471, 04014 (2024) TITDS-XIV-2023
8. Negmatov, S. S., Mamadoliev, K. M., Sobirov, B. B., Latipov, I. K., Ergashev, E., Rakhmanov, B. S., ... & Tajibaev, B. M. (2008, August). Improvement of physico-mechanical properties of thermoreactive and thermoplastic polymeric coverings by physical methods of modification. In AIP Conference Proceedings (Vol. 1042, No. 1, pp. 67-69). American Institute of Physics.
9. Rayimdjanova, O., Mukhtarov, F., Ismoilov, M. M., Abdusamatov, H., Abdullaeva, M., & Madaminov, M. Research of the semiconductor sensors based on anomal photovoltaic effect with highly sensitive parameters of the deformation. In E3S Web of Conferences (Vol. 508, p. 01004). EDP Sciences.https://doi.org/10.1051/e3sconf/202450801004
10. Kholmatov, U. S. (2022). STUDY OF A MATHEMATICAL MODEL OF A FIBER OPTIC SENSOR WITH LONGITUDINAL AND TRANSVERSE MOVEMENTS. SCIENTIFIC AND TECHNICAL JOURNAL OF MECHANICAL ENGINEERING, (1), 78-85.
11. [11]
12. Kholmatov, U. S. (2022). Determination of the basic theory of adaptive identification for the automation of multi-connected objects. SCIENTIFIC-TECHNICAL JOURNAL of Namangan Institute of Engineering Technology.–2022, 1(7), 544-550.
13. Rayimdjanova, O., Xatamova, Z., Rustamov, I., Xolmatov, S., Arabboyev, X., & Ibragimov, N. Z. Thermal converter for controlling horizontal wind speed and temperature. In E3S Web of Conferences (Vol. 508, p. 05004). EDP Sciences.

14. Umurzakova, D., Abdullayev, T., Khakimov, A., & Qadamova, Z. (2024, November). Development of automatic control system of drum boiler on the basis of fuzzy controller with pid-controller adaptation. In E3S Web of Conferences (Vol. 508, p. 01007). EDP Sciences.
15. Avazbekovich, I. N. (2022). Investigation Of The Influence Of Technological Factors Of Magnetic Treatment Of Polymer Coatings On Their Adhesion And Physical And Mechanical Properties. Journal of Pharmaceutical Negative Results, 1064-1070.
16. Igamberdiev, A. K., Muqimova, D. K., Usmanov, E. Z., & Usmanova, S. D. (2022). Influence of the thickness of the roller discs of the combined machine on the indicators of their work during the processing of plowed lands afterwards. In IOP Conference Series: Earth and Environmental Science (Vol. 954, No. 1, p. 012001). IOP Publishing.
17. Muqimova, D. K., Zingirov, S. J., Axmatohunov, B. M., Zokirov, D. Z., Melikuziev, A. R., & Tursunboev, L. E. (2024, October). The impact of the disc roller's diameter on the combined machine's performance during the sequential processing of freshly planted soil. In E3S Web of Conferences (Vol. 471, p. 04013).
18. Abdullayev, T., & Xoitqulov, A. (2024, March). Development of a mathematical model of a temperature calibrator. In AIP Conference Proceedings (Vol. 3045, No. 1). AIP Publishing.